IOP PUBLISHING JOURNAL OF PHYSICS: CONDENSED MATTER
J. Phys.: Condens. Matter **24** (2012) 455502 (6pp) doi:10.1088/0953-8984/24/45/455502

Modeling the radiation ionization energy and energy resolution of trigonal and amorphous selenium from first principles

A Darbandi[1,2], É Devoie[1,3], O Di Matteo[1,2] and O Rubel[1,2]

[1] Thunder Bay Regional Research Institute, 290 Munro St, Thunder Bay, ON, Canada
[2] Lakehead University, 955 Oliver Road, Thunder Bay, ON, Canada
[3] University of Waterloo, 200 University Avenue West, Waterloo, ON, Canada

E-mail: rubelo@tbh.net

Received 15 July 2012, in final form 1 October 2012
Published 19 October 2012
Online at stacks.iop.org/JPhysCM/24/455502

Abstract
Advances in the development of amorphous selenium-based direct conversion photoconductors for high-energy radiation critically depend on the improvement of its sensitivity to ionizing radiation, which is directly related to the pair production energy. Traditionally, theories for the pair production energy have been based on the parabolic band approximation and do not provide a satisfactory agreement with experimental results for amorphous selenium. Here we present a calculation of the pair creation energy in trigonal and amorphous selenium based on its electronic structure. In indirect semiconductors, such as trigonal selenium, the ionization threshold energy can be as low as the energy gap, resulting in a lower pair creation energy, which is a favorable factor for sensitivity. Also, the statistics of photogenerated charge carriers is studied in order to evaluate the theoretical value of the Fano factor and its dependence on recombination processes. We show that recombination can significantly compromise the detector's energy resolution as a result of an increase in the Fano factor.

(Some figures may appear in colour only in the online journal)

1. Introduction

Semiconductors are widely used as functional materials in high-energy radiation detectors, including amorphous selenium-based flat-panel x-ray detectors [1] and (CdZn)Te detectors, with applications in medical and industrial imaging [2, 3], dosimetry and security [4]. The sensitivity of these detectors is determined by their ability to convert high-energy photons into electron–hole pairs. The corresponding characteristic of the material is the pair creation energy, $W_{\pm}^{0}$, which is the ratio between the radiation ionization energy and the average number of electron–hole pairs created (quantum yield).

The theory of electron–hole pair production by impact ionization in semiconductors was initially introduced by Shockley [5] and further refined by Klein [6] in the context of electron–hole pair generation by ionizing radiation. According to Klein [6], $W_{\pm}^{0}$ is related to the semiconductor energy gap E_g, the average residual kinetic energy of resultant carriers $\langle E_k \rangle$, and the average energy loss to optical phonons $\langle E_{ph} \rangle$ between two ionization events in the following way

$$W_{\pm}^{0} = E_g + 2\langle E_k \rangle + \langle E_{ph} \rangle. \quad (1)$$

The factor of 2 above accounts for the residual excess energy of both resultant charge carriers (electron and hole). Considering energy and momentum conservation requirements during the pair production event [7] and assuming a parabolic band dispersion along with the random-**k** approximation [8], the following expression is obtained for the pair creation energy [6]

$$W_{\pm}^{0} \approx 2.8E_g + \langle E_{ph} \rangle. \quad (2)$$

The average phonon energy loss is usually assumed to be in the range of $\langle E_{\rm ph}\rangle = 0.5$–1 eV for the majority of semiconductors [5].

In spite of the number of approximations involved, equation (2) provides a good representation of the experimentally observed linear dependence of $W_{\pm}^{0}$ on the energy gap in most semiconductors [6]. The notable exception is amorphous selenium (a-Se), for which equation (2) overestimates the pair creation energy by approximately 2 eV [9]. In particular, the mobility gap of a-Se is about 2.3 eV [10], which, through equation (2), leads to the theoretical $W_{\pm}^{0} \approx 7.0$–7.5 eV. However, the experimental intrinsic value of $W_{\pm}^{0}$ in a-Se is approximately 4–6 eV [11].

Que and Rowlands [9] proposed to resolve this inconsistency in a-Se by assuming that the ionization threshold energy, $E_{\rm th}$, is equal to the energy gap. This assumption implies loosening the requirement of momentum conservation, which is motivated by the disordered structure of a-Se. Accordingly, equation (2) is transformed into [5, 9]

$$W_{\pm}^{0} \approx 2.2E_{\rm g} + \langle E_{\rm ph}\rangle. \tag{3}$$

The latter expression is consistent with the experimental data for the pair production energy in a-Se.

Recent analysis of the electronic structure of trigonal selenium (t-Se) indicates that $E_{\rm th} \approx E_{\rm g}$ for both types of charge carriers as a result of the indirect band structure [12]. Therefore, the assumption regarding violation of momentum conservation is not necessarily required for interpretation of the low $W_{\pm}^{0}$ in a-Se.

In this paper, we report detailed calculations of the electron–hole pair creation energy in t-Se and a-Se from first principles. Unlike previous calculations [9], which were based on the parabolic band structure approximation, our calculations include realistic density of states (DOS) and ionization threshold energies that result in more accurate and reliable prediction of the pair creation energy. Furthermore, we report theoretical values of the Fano factor, a measure of the dispersion of the probability distribution of $W_{\pm}^{0}$. The calculated intrinsic Fano factor turns out to be lower than that in (CdZn)Te, indicating a high potential for the energy resolution in both t-Se and a-Se. In the discussion, we specially emphasize the statistical role of recombination as a limiting factor of the energy resolution.

2. Calculation method

The generation of charge carriers by ionizing radiation is generally viewed as a two-step process. The first step involves the absorption of a high-energy photon and the subsequent creation of primary energetic electrons and holes. In the second step, the primary charge carriers lose their kinetic energy mainly by impact ionization, leading to the production of secondary electron–hole pairs. The process continues until the excess kinetic energy of the secondary carriers falls below the ionization threshold. The main challenge in theoretical calculation of the pair production energy using equation (1) is finding an accurate approximation for the average kinetic energy of residual charge carriers while taking into account the electronic structure of the material in question.

Here we use a random-**k** approximation, which has proven to be successful especially for transitions far from the ionization threshold [8, 13]. This approximation implies a uniform distribution of final carriers in **k**-space, which translates into the probability for a resultant carrier of falling in the energy interval $(E, E + {\rm d}E)$ to be proportional to the density of states $\rho(E)$. The average kinetic energy of residual electrons can then be expressed as [7]

$$\langle E_{\rm k,e}\rangle = \frac{\int_{E_{\rm CBM}}^{E_{\rm th,e}} (E - E_{\rm CBM})\rho(E)\,{\rm d}E}{\int_{E_{\rm CBM}}^{E_{\rm th,e}} \rho(E)\,{\rm d}E}, \tag{4}$$

where $E_{\rm th,e}$ is the ionization threshold energy for electrons and $E_{\rm CBM}$ is the energy position of the conduction band minimum. It is straightforward to extend equation (4) for holes, therefore we omit it here.

Calculation of DOS for trigonal selenium (t-Se) was undertaken in the framework of the density functional theory implemented in the `ABINIT` package [14, 15]. The generalized gradient approximation (GGA) [16] and Troullier–Martins pseudopotentials [17, 18] were employed. The valence electron wavefunctions were expanded using a plane-wave basis set with a cutoff energy of 25 Ha. The Brillouin zone was sampled using a Monkhorst–Pack [19] $20 \times 20 \times 18$ **k**-point mesh. Further details regarding the geometry of the model structure and convergence criteria have been reported elsewhere [12, 20].

DOS for the amorphous phase was also calculated from first principles. The simulation cell consists of 50 atoms placed in a cubic supercell with periodical boundary conditions. The creation of the a-Se structure involves two steps. First, a preliminary structure of a-Se was created using a self-avoiding random-walk model (also known as a disordered chain model) [21–23]. In this model, the chains of atoms are built by arranging atoms such that the nearest-neighbor distances and the bond angles correspond to the equilibrium experimental values, while the dihedral angle between atoms in the same chain is random. Second, the structural relaxation was performed using a full-potential linearized augmented plane-wave method implemented in the `WIEN2k` package [24] and GGA [16] for the exchange–correlation functional. The energy to separate core and valence electrons was set to -6 Ryd. The product of the atomic sphere radius and plane-wave cutoff in k-space was equal to 7. The Brillouin zone was sampled using a $2 \times 2 \times 2$ Monkhorst–Pack mesh [19]. The internal degrees of freedom were relaxed by minimizing the total energy and forces acting on atoms. In the final structure, the residual forces did not exceed 2 mRyd/Bohr.

The DFT energy gap of t-Se is about 1 eV, which is significantly underestimated with respect to the experimental value of 1.85 eV [25–27]. This inconsistency is attributed to a well-known shortcoming of explicit density-dependent functionals, which tend to underestimate the energy gap [28]. In the following analysis, the so-called 'scissor operator' (energy offset) was applied in order to match the theoretical

energy gap with its experimental value. The same energy offset was also applied when calculating DOS for a-Se.

The Fano factor was calculated from the variance σ_N^2 in the number N of electron–hole pairs generated per incident high-energy photon absorbed as follows [29]

$$F = \frac{\sigma_N^2}{\langle N \rangle}. \tag{5}$$

The statistics of electron–hole pair generation was modeled using a Monte Carlo simulation algorithm based on random values of $W_{\pm}^0$ and a fixed energy $\hbar\omega_0$ of the absorbed photon. The calculations were performed for the photon energy of 10 and 100 keV, but no noticeable difference in the value of Fano factor was found.

Random values of the electron–hole pair creation energy were determined according to

$$W_{\pm}^0 = E_g + E_{k,e} + E_{k,h} + r\hbar\omega_{op}. \tag{6}$$

Here $E_{k,e}$ and $E_{k,h}$ are the electron and hole kinetic energies taken randomly in the range 0–E_{th} with a probability distribution proportional to the density of states $\rho(E)$ in the conduction and valence band, respectively. The stochastic nature of energy loss due to the optical phonon emission is taken into account via a random number of phonons emitted r with the exponential distribution

$$p(r) = \langle r \rangle^{-1} e^{-r/\langle r \rangle}, \tag{7}$$

where $\langle r \rangle$ represents the average number of phonons emitted per electron–hole pair produced.

Using a set of random values $W_{\pm}^0(i)$, the number of electron–hole pairs N generated per incident photon was determined from the following condition

$$0 \leq \left[\sum_{i=1}^{N} W_{\pm}^0(i) \right] - \hbar\omega_0 < W_{\pm}^0(N). \tag{8}$$

After multiple realizations, we build a statistically viable set of data that allows evaluation of the Fano factor using equation (5).

3. Results and discussion

3.1. Pair creation energy

We begin the calculation of the average pair creation energy $W_{\pm}^0$ by identifying the values of its main constituents: the semiconductor energy gap E_g, the average residual kinetic energy of resultant carriers $\langle E_k \rangle$ and the average energy loss to optical phonons $\langle E_{ph} \rangle$.

The energy gap of t-Se is 1.85 eV [25–27]. In amorphous structures, E_g is not well defined due to the extended band tails. Therefore, we use a range of 1.95–2.3 eV for a-Se. The lower bound corresponds to optical absorption measurements [30, 31], whereas the upper limit is set by transport measurements of the mobility gap [10, 32, 33].

Calculation of the average kinetic energy for residual carriers requires knowledge of the DOS near the top of the valence band and the bottom of the conduction band, as well as the ionization threshold. The calculated DOSs of t-Se and a-Se are presented in figure 1. Both DOSs clearly exhibit the presence of bonding, antibonding and lone-pair states. The width of the corresponding bands is about 2.5–3 eV, which is consistent with previous calculations [34, 35] and experimental measurements [36, 37]. The lone-pair DOS of t-Se has a characteristic double-peak structure [34, 35], which is well reproduced in our calculations. In the case of a-Se, peaks and the band edges are smeared due to the disorder [37]. Nevertheless, it is still possible to resolve a gap between bonding and antibonding DOS, the presence of which is a signature of a distorted, but not random dihedral angle [35, 38]. Some sharp features are still present in a-Se DOS (figure 1) and can be related to the finite size of the simulation volume. However, the latter does not affect the calculation of $W_{\pm}$ due to the averaging procedure in equation (4).

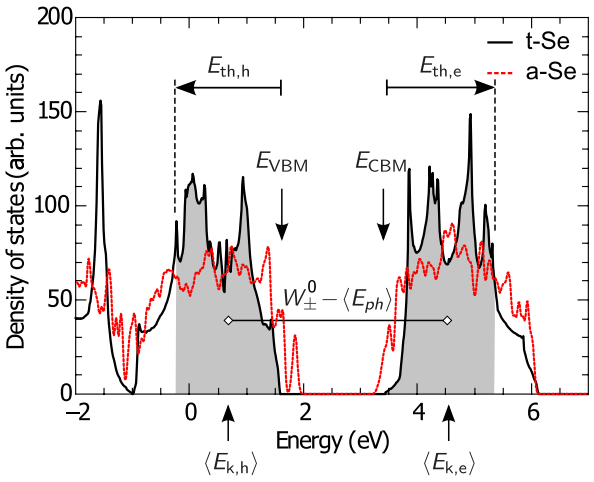

Figure 1. Density of states in t-Se (black solid line) calculated using DFT. The top of the valence band and bottom of the conduction band are marked as E_{VBM} and E_{CBM}, respectively. The shaded area indicates the states that can be occupied by residual charge carriers with excess energy not exceeding the ionization threshold energy for electrons and holes ($E_{th,e}$ and $E_{th,h}$, respectively). The center of mass of the shaded area corresponds to the average kinetic energy $\langle E_k \rangle$ of residual carriers. The difference between these energies is the pair creation energy minus the phonon contribution, $W_{\pm}^0 - \langle E_{ph} \rangle$. The calculated DOS for a-Se is shown for comparison (red dashed line). The Gaussian broadening of 25 meV was applied in both cases.

The threshold energies for electrons and holes are derived from analysis of the t-Se band structure taking into account energy and momentum conservation requirements [12]. The results of the calculation suggest that the ionization threshold in t-Se is approximately equal to the energy gap ($E_{th,e} = E_g$ and $E_{th,h} = 1.05E_g$ [12]). This result differs significantly from that predicted by the parabolic band approximation ($E_{th} = 1.5E_g$) and can be attributed to the indirect band structure of t-Se.

Using the ionization threshold energies and the calculated DOS function $\rho(E)$ for t-Se and a-Se, we calculate the average kinetic energy for residual carriers as a weighted average of the shaded regions in figure 1 (shown for t-Se DOS only). Using equation (4) we obtain the ratio $\langle E_k \rangle / E_g = 0.54 \pm 0.04$.

Table 1. Intrinsic pair creation energy (eV) in t-Se/a-Se assuming various values of the energy gap and the average number $\langle r \rangle$ of optical phonons emitted.

	Energy gap (eV)		
$\langle r \rangle$	1.85	2.1	2.3
10	4.4/—	4.7/4.4	5.0/4.5
20	4.7/—	5.0/4.7	5.3/4.8
30	5.0/—	5.3/5.0	5.6/5.1

Table 2. Intrinsic Fano factor for t-Se/a-Se assuming various values of the energy gap.

	Energy gap (eV)		
$\langle r \rangle$	1.85	2.1	2.3
10	0.036/—	0.031/0.044	0.030/0.043
20	0.044/—	0.038/0.051	0.036/0.049
30	0.057/—	0.050/0.063	0.046/0.059

Here the margins appear due to the uncertainty of the band gap energies. The difference between the average kinetic energy for electrons and holes is marginal and it does not exceed the error-bar. It should be noted that the obtained average kinetic energy is much less than that predicted by the parabolic band approximation $\langle E_k \rangle / E_g = 0.9$. The difference is largely attributed to the fact that $E_{th} \approx E_g$.

The average energy loss due to phonon emission $\langle E_{ph} \rangle$ between two successive ionization events can be estimated based on the average number of phonons emitted $\langle r \rangle$ and the optical phonon energy $\hbar\omega_{op}$. According to [5], $\langle r \rangle$ is not sensitive to the material composition and ranges between 10 and 30. The phonon spectra of trigonal and amorphous selenium phases are very similar [39] with the high-energy peak at 29 and 31 meV for t-Se and a-Se, respectively [40]. In our calculation we take the value of $\hbar\omega_{op} = 30$ meV, which results in the average energy loss to phonons $\langle E_{ph} \rangle =$ 0.3–0.9 eV.

The pair creation energies in t-Se and a-Se calculated according to equation (1) are presented in table 1. The expectation value of $W_{\pm}^0$ ranges between 4.4 and 5.6 eV depending on the choice of material parameters, E_g and $\langle r \rangle$. The difference between the values of $W_{\pm}^0$ for a-Se and t-Se is marginal (about 10%), and it can be attributed to a more uniform DOS of a-Se (figure 1). These data correspond to the *intrinsic* pair creation energy implying that the electron–hole pair generation and collection is not mediated by recombination or incomplete energy absorption (such as Compton scattering). The theoretical values of $W_{\pm}^0$ agree with those measured experimentally for a-Se: $W_{\pm}^0 =$ 4–6 eV [11], 6 eV [41, 42], 5.4 eV [43]. The results of our detailed calculations are remarkably close to those obtained using the approximate equation (3) that explains the success of Que and Rowlands [9] analysis of x-ray photogeneration in a-Se with the assumption that $E_g = E_{th}$. However, the violation of momentum conservation is not required in our case.

3.2. Fano factor

Fluctuations in the number of charge carriers generated as a result of absorption of a high-energy radiation can be expressed through the Fano factor. It is closely related to the intrinsic limit of the energy resolution of the detector [4, p 377]. We proceed with calculation of the Fano factor according to its definition in equation (5) using the same parameters as for the pair creation energy. The results are presented in table 2.

Our calculations suggest that the intrinsic value of the Fano factor in t-Se and a-Se is in the range of 0.03–0.06. The Fano factor increases with decreasing energy gap E_g and increasing number of phonons $\langle r \rangle$ emitted between two consequent pair production events. The disparity between a-Se and t-Se values of the Fano factor is practically negligible and can be assigned to a broader distribution of energy of resultant carriers in the case of a-Se. It is apparent that the Fano factor in t-Se and a-Se is superior to the corresponding value in such technologically prevalent semiconductors as Ge, Si and (CdZn)Te, where the Fano factor amounts to 0.059, 0.067 and 0.089, respectively [44, 45].

One should bear in mind that the intrinsic values of the Fano factor can only be observed under the circumstances of complete collection of photogenerated charge carriers. Recombination and charge trapping are two major mechanisms that limit the collection efficiency in a-Se [9, 42, 46]. Even at a relatively strong electric field of 10 V μm^{-1}, only about 10% of photogenerated carriers survive recombination, which is evident from the high value of the pair creation energy $W_{\pm} \approx 40$ eV [47] compared to the intrinsic value of $W_{\pm}^0 \approx 5$ eV.

Provided recombination is the only stochastic factor that governs variation in the number N of electron–hole pairs created, statistics of the charge conversion are then described by a binomial distribution with the variance of $Np(1-p)$ and mean $N(1-p)$, where p is the recombination probability. Hence, according to equation (5), the Fano factor is given by $F = p$. This simple result sets the lower statistical limit for the Fano factor due to recombination.

In order to account for recombination as an additional source of variance in the number of electron–hole pairs generated, we include the recombination probability p as a parameter into the Monte Carlo algorithm for the calculation of the Fano factor. The simulated dependence of the Fano factor on the recombination probability is presented in figure 2. In the limit of small recombination probabilities, the Fano factor approaches its intrinsic value F_0. The Fano factor then deteriorates progressively, approaching the limit of $F = p$, as the fraction of the carriers that recombine increases.

Using a heuristic approach, we derived a general expression for the Fano factor

$$F = F_0(1-p) + p \tag{9}$$

that captures both effects: statistical fluctuations of the pair creation energy included in the intrinsic Fano factor F_0 and the carrier loss due to recombination. Equation (9) successfully

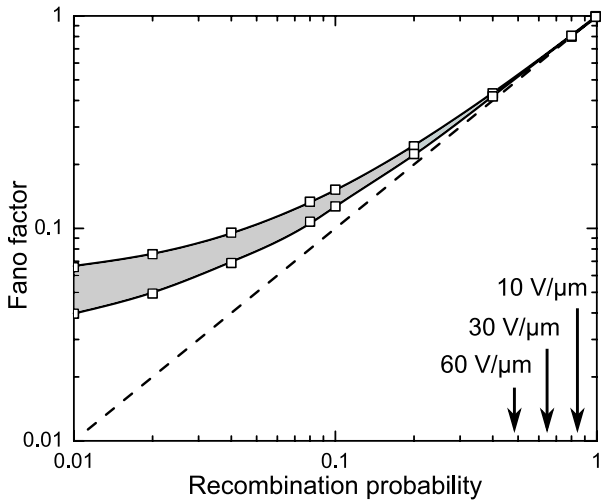

Figure 2. Dependence of the Fano factor on the recombination probability in a-Se calculated using Monte Carlo simulation (symbols) and analytically using equation (9). The shaded region represents the uncertainty in the intrinsic value of the Fano factor according to the range of data in table 2. The dashed line corresponds to the recombination-limited value of the Fano factor $F = p$. The arrows indicate an approximate value of the recombination probability taken from [9, 47] for the specified electric fields.

reproduces results of the Monte Carlo simulation as shown in figure 2.

Our analysis suggests that the nearly intrinsic value of the Fano factor can only be achieved if one manages to keep the recombination probability below 0.1 for a-Se, or more generally $p \lesssim F_0$. In practice, the recombination can be controlled by the strength of an external electric field applied to the sample. The pulse height spectroscopy experiments performed on a-Se at a field of 20 V μm^{-1} indicate a broad distribution of Ns [47, 48], which is consistent with the recombination-limited statistics. Apparently, electric fields much greater than 60 V μm^{-1} are required in order to lower the Fano factor down to its intrinsic limit (see figure 2).

In the case of single photon detectors when the energy of the incident radiation is concerned, the most important factor is the energy resolution, which is given by [49, p 118]

$$R = 2.35\sqrt{F/\langle N\rangle}. \tag{10}$$

Apparently, the lower Fano factor of the photoconductor directly translates into a better energy resolution of the detector. However, when the detector operates in the integration mode, one of the main performance factors is the detective quantum efficiency [50, p 26]. The latter is proportional to the Swank factor A_S, which also depends on the Fano factor and the average number $\langle N\rangle$ of electron–hole pairs collected

$$A_S = \frac{\langle N\rangle}{F + \langle N\rangle}. \tag{11}$$

Given that the number of created charge carriers is much greater than the Fano factor, A_S in a-Se comes very close to unity [48, 51], its ideal value. In this case, the Fano factor does not play a significant role in determining the detector characteristics.

4. Conclusions

The objective of our theoretical study was the calculation of the charge pair production energy and the Fano factor in t-Se and a-Se. The calculation was based on the electronic structure of t-Se and a-Se, which was obtained self-consistently from first principles in the framework of a density functional theory. The statistics of the electron–hole pair generation were modeled using a Monte Carlo simulation technique and a random-**k** approximation to determine the final state of resultant charge carriers.

Results of our calculations suggest that the intrinsic theoretical value of the pair creation energy $W_{\pm}^0$ in a-Se and t-Se ranges between 4.4 and 5.6 eV. The value is practically insensitive to the structural order of selenium. The uncertainty is related to the flexibility in the choice of material parameters, such as the energy/mobility gap and the average number of phonons emitted between two consequent pair production events. Obtained values agree well with experimental data available in the literature for a-Se. The puzzling overestimation of $W_{\pm}^0$ by Klein's traditional formula is attributed to a relatively low average kinetic energy of resultant charge carriers. This observation is closely related to low ionization threshold energies for both charge carriers in t-Se as a consequence of its indirect band structure. Our interpretation provides an alternative to violation of the momentum conservation, which was put forward previously in the literature to explain the deviation of $W_{\pm}^0$ from Klein's formula.

According to theoretical predictions, the intrinsic value of the Fano factor F_0 in selenium is confined within the range of 0.03–0.06, which is superior to the corresponding characteristic in Si, Ge and (GdZn)Te. However, achieving these values practically can be challenging due to the recombination of photogenerated charge carriers, which is present to a large extent in selenium even at strong electric fields (10–60 V μm^{-1}). We propose a correction to the Fano factor that takes into account the effect of the carrier loss due to recombination. The analysis suggests that the nearly intrinsic value of the Fano factor can only be achieved, when the recombination probability is reduced below F_0. Otherwise, the Fano factor and, correspondingly, the energy resolution of a detector is limited by a recombination statistics rather than by fluctuations in the pair creation energy.

Acknowledgments

The financial support of the Natural Sciences and Engineering Research Council of Canada under a Discovery Grants Program 'Microscopic theory of high-field transport in disordered semiconductors', Ontario Ministry of Research and Innovation through a Research Excellence Program 'Ontario network for advanced medical imaging detectors' and Thunder Bay Community Economic and Development Commission is gratefully acknowledged.

References

[1] Rowlands J and Kasap S 1997 *Phys. Today* **50** 23
[2] Eisen Y, Shor A and Mardor I 1999 *Nucl. Instrum. Methods* A **428** 158
[3] Scheiber C and Giakos G 2001 *Nucl. Instrum. Methods* A **458** 12
[4] Knoll G 1979 *Radiation Detection and Measurement* (New York: Wiley)
[5] Shockley W 1961 *Solid-State Electron.* **2** 35
[6] Klein C A 1968 *J. Appl. Phys.* **39** 2029
[7] Alig R C and Bloom S 1975 *Phys. Rev. Lett.* **35** 1522
[8] Kane E O 1967 *Phys. Rev.* **159** 624
[9] Que W and Rowlands J A 1995 *Phys. Rev.* B **51** 10500
[10] Juska G 1991 *J. Non-Cryst. Solids* **137–138** 401
[11] Kasap S O, Aiyah V, Polischuk B and Baillie A 1998 *J. Appl. Phys.* **83** 2879
[12] Darbandi A and Rubel O 2012 *J. Appl. Phys.* submitted, arXiv:1210.4119 [cond-mat.mtrl-sci]
[13] Geist J and Gladden W K 1983 *Phys. Rev.* B **27** 4833
[14] Gonze X *et al* 2002 *Comput. Mater. Sci.* **25** 478
[15] Gonze X *et al* 2005 *Z. Kristallogr.* **220** 558
[16] Perdew J P, Burke K and Ernzerhof M 1996 *Phys. Rev. Lett.* **77** 3865
[17] Troullier N and Martins J L 1991 *Phys. Rev.* B **43** 1993
[18] Fuchs M and Scheffler M 1999 *Comput. Phys. Commun.* **119** 67
[19] Monkhorst H J and Pack J D 1976 *Phys. Rev.* B **13** 5188
[20] Darbandi A and Rubel O 2012 *J. Non-Cryst. Solids* **358** 2434
[21] Misawa M and Suzuki K 1978 *J. Phys. Soc. Japan* **44** 1612
[22] Bellissent R and Tourand G 1980 *J. Non-Cryst. Solids* **1221** 35–6
[23] Balasubramanian S, Damodaran K and Rao K 1992 *Chem. Phys.* **166** 131
[24] Blaha P, Schwarz K, Madsen G K H, Kvasnicka D and Luitz J 2001 *Wien2k: An Augmented Plane Wave + Local Orbitals Program for Calculating Crystal Properties* (Wien: Karlheinz Schwarz, Techn. Universität)
[25] Fischer R 1972 *Phys. Rev.* B **5** 3087
[26] Moreth B 1979 *Phys. Rev. Lett.* **42** 264
[27] Takumi M, Tsujioka Y, Hirai N, Yamamoto K and Nagata K 2010 *J. Phys.: Conf. Ser.* **215** 012049
[28] Perdew J P 1985 *Int. J. Quantum Chem.* **28** 497
[29] Fano U 1947 *Phys. Rev.* **72** 26
[30] Tichỳ L, Tichá H, Nagels P, Sleeckx E and Callaerts R 1996 *Mater. Lett.* **26** 279
[31] Solieman A and Abu-Sehly A 2010 *Physica* B **405** 1101
[32] Vanhuyse B, Grevendonk W, Adriaenssens G J and Dauwen J 1987 *Phys. Rev.* B **35** 9298
[33] Abkowitz M 1988 *Philos. Mag. Lett.* **58** 53
[34] Joannopoulos J D, Schlüter M and Cohen M L 1975 *Phys. Rev.* B **11** 2186
[35] Bullett D W 1975 *J. Phys. C: Solid State Phys.* **8** L377
[36] Nielsen P 1972 *Phys. Rev.* B **6** 3739
[37] Ono I, Grekos P C, Kouchi T, Nakatake M, Tamura M, Hosokawa S, Namatame H and Taniguchi M 1996 *J. Phys.: Condens. Matter* **8** 7249
[38] Hohl D and Jones R O 1991 *Phys. Rev.* B **43** 3856
[39] Gompf F 1981 *J. Phys. Chem. Solids* **42** 539
[40] Poborchii V V, Kolobov A V and Tanaka K 1998 *Appl. Phys. Lett.* **72** 1167
[41] Haugen C, Kasap S O and Rowlands J 1999 *J. Phys. D: Appl. Phys.* **32** 200
[42] Kasap S 2000 *J. Phys. D: Appl. Phys.* **33** 2853
[43] Lachaine M and Fallone B 2000 *J. Phys. D: Appl. Phys.* **33** 1417
[44] Papp T, Lepy M -C, Plagnard J, Kalinka G and Papp-Szabo E 2005 *X-Ray Spectrom.* **34** 106
[45] Redus R H, Pantazis J A, Huber A C, Jordanov V T, Butler J F and Apotovsky B 1997 *MRS Proc.* vol 487, p 101
[46] Fang Y, Badal A, Allec N, Karim K and Badano A 2012 *Med. Phys.* **39** 308
[47] Blevis I M, Hunt D C and Rowlands J A 1999 *J. Appl. Phys.* **85** 7958
[48] Blevis I M, Hunt D C and Rowlands J A 1998 *Med. Phys.* **25** 638
[49] Leo W R 1994 *Techniques for Nuclear and Particle Physics Experiments* (Berlin: Springer)
[50] Gevenois P and Bankier A 2004 *Imaging* (Sheffield: European Respiratory Society)
[51] Kasap S O and Rowlands J A 2002 *Proc. IEEE* **90** 591